Journal of
Materials Chemistry A

Accepted Manuscript

This article can be cited before page numbers have been issued, to do this please use: S. Wannapaibooon, K. Sumida, K. Dilchert, M. Tu, S. Kitagawa, S. Furukawa and R. A. A. Fischer, *J. Mater. Chem. A*, 2017, DOI: 10.1039/C7TA02848B.

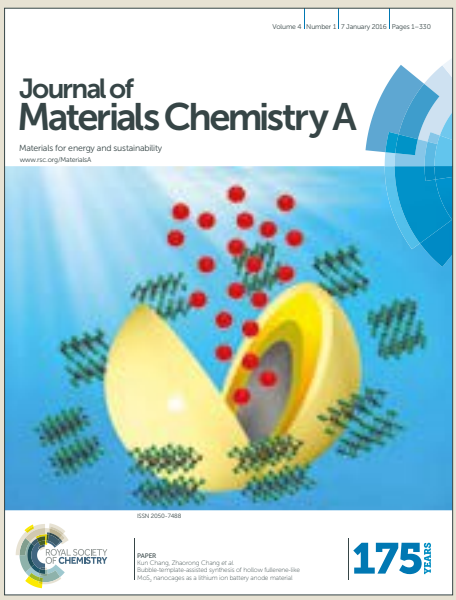

ROYAL SOCIETY OF CHEMISTRY

rsc.li/materials-a

View Article Online
DOI: 10.1039/C7TA02848B

Journal of Materials Chemistry A

ARTICLE

Enhanced Properties of Metal-Organic Framework Thin-Films Fabricated via a Coordination Modulation-Controlled Layer-by-Layer Process

Received 00th January 20xx,
Accepted 00th January 20xx

DOI: 10.1039/x0xx00000x

www.rsc.org/

Suttipong Wannapaiboon,[a,b] Kenji Sumida,[c,d,*] Katharina Dilchert,[b] Min Tu,[b,e] Susumu Kitagawa,[c] Shuhei Furukawa[c] and Roland A. Fischer[a,*]

One of the primary challenges facing the integration of metal-organic frameworks (MOFs) with real-world technologies is the development of enhanced fabrication processes that maximize compatibility with specific device configurations, while maintaining or even improving the performance profile relative to bulk MOF materials. Stepwise liquid-phase epitaxy (LPE) has emerged as an important method for depositing MOF thin-films on variety of substrate types, although current limitations include challenges in obtaining well-oriented and highly-crystalline thin-films, and the applicability of the technique beyond the most common MOF structure types (e.g. paddlewheel-based MOFs). Coordination modulation is a method often employed for controlling MOF crystal growth processes within bulk crystallization solutions, and presents a potentially powerful route for manipulation of the properties of MOF thin-films via integration to a LPE-based process. In this work, the coordination modulation is employed in the LPE fabrication of thin-films composed of the $Zn_4O(L)_3$ structure type (L^{2-} = 3,5-dialkyl-4-carboxypyrazolate). The films are grown on Au-coated quartz crystal microbalance (QCM) substrates, allowing both film deposition and molecular adsorption to be precisely probed. Addition of a modulator during the LPE process leads to enhanced orientation and crystallinity that offer a boost in adsorption capacities of polar adsorbates when using small molar ratio of the modulator. Closer inspection of the QCM data reflects a change in growth kinetics, which influences the quantity of MOF deposited per growth cycle and the overall growth rate. In all, this integrated fabrication process could provide a potentially versatile route for the fabrication of a wide range of MOF thin-films with enhanced characteristics.

Introduction

Metal-organic frameworks (MOFs) are a novel class of microporous solid assembled from metal-based nodes and organic bridging linkers to form infinite, microporous crystalline networks.[1] The tremendous diversity of components that can be used to construct these materials provides opportunities for precise, bottom-up design of both the framework structure and the chemical properties of the pore surfaces.[2] This versatility has led to their investigation in a variety of potential applications, including gas storage,[3] molecular separations,[4] and heterogeneous catalysis.[5] Moreover, the potential to incorporate MOFs within functional devices has resulted in their investigation with respect to a wide variety emerging applications, including electronics and optoelectronics,[6] proton conduction,[7] photocatalysis,[8] sensing,[9] optics,[10] and biomolecular and drug delivery.[11] Here, one of the primary challenges is the development of enhanced fabrication techniques that allow MOFs to be structuralized into meso- and macroscopic forms that are compatible with the specific configuration of the device.[12] Further, a more detailed knowledge regarding the influence of such processing on the properties of MOFs is needed in order to ensure that the performance profile of the bulk material is maintained (or even improved upon) under real-world operation conditions.

In the area of MOF thin-film deposition, *liquid-phase epitaxy* (LPE, or *layer-by-layer deposition*) has emerged as an important method for depositing films on a variety of substrate types. In this technique, solutions containing the metal ion source and organic linkers are alternatingly provided to a crystal growth surface to allow the MOF to grow with a well-controlled film thickness and surface coverage by setting the number of growth cycles associated with the deposition process.[13] Although the utility of this technique has been demonstrated via the successful deposition of several MOF systems,[13] well-controlled film growth and crystal orientation has remained elusive to date

[a] Chair of Inorganic and Metal-Organic Chemistry, Technical University of Munich, Lichtenbergstr. 4, D-85748 Garching, Germany. Fax: +49(0) 89-289-13194; Tel: +49(0) 89-289-13081; *E-mail: roland.fischer@tum.de
[b] Chair of Inorganic Chemistry II, Ruhr-University Bochum, Universitaetstr. 150, D-44801 Bochum, Germany.
[c] Institute for Integrated Cell-Material Sciences (WPI-iCeMS), Kyoto University, Yoshida, Sakyo-ku, 606-8501 Kyoto, Japan.
[d] Centre for Advanced Nanomaterials, School of Physical Sciences, The University of Adelaide, SA 5005, Australia; *E-mail: kenji.sumida@adelaide.edu.au
[e] Center for Surface Chemistry and Catalysis, Katholieke Universiteit Leuven, Celestijnenlaan 200f – box 2461, 3001 Leuven, Belgium.
Electronic Supplementary Information (ESI) available: [details of any supplementary information available should be included here]. See DOI: 10.1039/x0xx00000x

for MOF systems beyond the paddlewheel-based MOFs.[14] Moreover, little attention has been directed toward understanding the underlying mechanisms allowing for fine-tuning of the crystal growth processes in order to achieve even greater control over the quality of the resulting films. Specifically, the application of synthetic strategies known to manipulate the growth of bulk MOF crystals with respect to thin-film fabrication protocols, and the elucidation of how such processing can influence the performance of the resulting films would greatly advance the prospects for the use of MOF-based thin-films in the types of applications mentioned above.

Among the synthetic methods available for controlling the growth of MOF crystals, the *coordination modulation* technique is particularly effective in providing control over the resulting crystal size and the crystal morphology. Here, the addition of a coordination modulator, which typically bears the same coordinating functional group as the organic linker used to construct the framework (e.g. a carboxylate moiety), gives rise to competitive phenomena in solution that influences both the crystal nucleation and growth processes.[15] The extent to which these processes are affected can be controlled via the coordinating strength of the modulator, as well as through the quantity introduced to the reaction mixture. Indeed, a systematic and rational control over the crystal size across the nanometer-to-micrometer size regimes has been demonstrated in a variety of systems.[16-23] The broad applicability of this approach in bulk MOF syntheses suggests that it could similarly be a powerful tool for enhancing the quality and properties of MOF thin-films.[24]

In the present work, we explore the use of the coordination modulation technique in an LPE-based process, with an object of assessing its potential utility in enhancing the quality and performance of MOF-based thin-films. Specifically, the $Zn_4O(L)_3$ (**Zn-L**) structure type[24] (L^{2-} = 3,5-dialkyl-4-carboxypyrazolate, Fig. 1) has been selected for further study due to its previous success in being processed via a conventional LPE route. It is found that the addition of an acetic acid modulator significantly influences the crystallinity of the **Zn-L** material obtained from bulk crystallization solutions, and further, when used in conjunction with LPE, it also enhances the preferred orientation of the product thin-films. Variation of the modulator concentration is also shown to influence the quantity of the films deposited on the substrate surface, likely due to manipulation of the equilibrium between free metal clusters in solution and those bound to the growth surface (which in turn contribute to construction of further MOF layers). The enhanced film crystallinity is further reflected by a boosted adsorption capacity of polar adsorbates, confirming that coordination modulation can assist in the fabrication of higher-quality MOF thin-films.

Experimental

Fabrication of MOF films

The surface of Au-coated QCM sensors (Q-Sense, AT cut type, Au electrode, diameter 14 mm, thickness 0.3 mm, and fundamental frequency ca. 4.95 MHz) were functionalized by self-assembled monolayer (SAM) of 16-mercaptohexadecanoic acid (MHDA) prior to the MOF film fabrications. Three different MOF films (**Zn-DM**, **Zn-ME** and **Zn-DE**, precursors are listed in Table S1) were fabricated via integration of coordination modulation with LPE process for 45 cycles at controlled temperature of 40°C using an automated QCM instrument (Q-Sense E4 Auto) operated in the continuous flow mode with a flow rate of 100 μL min^{-1}. Note that, the materials were grown

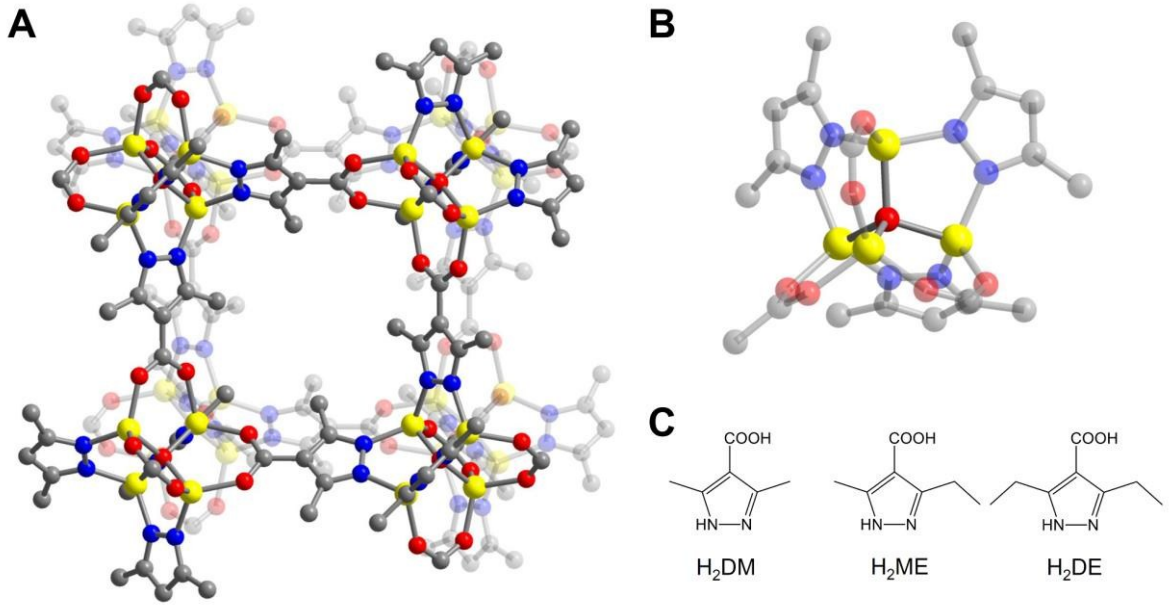

Fig. 1 (A) A portion of the single-crystal structure of $Zn_4O(DM)_3$ (**Zn-DM**) as viewed along the crystallographic *a*-axis; (B) an enlarged view of a $[Zn_4O]^{6+}$ unit within the structure; and (C) molecular structures of the three organic linkers employed in this work. Yellow, gray, blue, and red spheres represent Zn, C, N, and O atoms, respectively. Note that, in panels A and B, hydrogen atoms and the disorder in the orientation of the linkers has been omitted for clarity.

on the QCM substrates to allow real-time monitoring of the deposition process as well as a detailed characterization of the adsorption properties of each fabricated film. Acetic acid was used as modulator and mixed with the $Zn_4O(OAc)_6$ solution with controlled molar ratio. In each deposition cycle, the functionalized QCM substrate was alternatingly exposed to the precursor solutions as follow: $Zn_4O(OAc)_6$ mixed with acetic acid 10 min, ethanol (solvent) 5 min, organic linker 10 min and finally ethanol 5 min. The modulator-to-metal ratio were varied ranging from 1 to 5. Moreover, the LPE-based MOF films fabricated without using modulator were use as the control experiments.

Characterization methods

The crystalline phase and crystal orientation of the obtained MOF thin-films were identified by powder X-ray diffraction (PXRD, X'Pert PanAnalytical instrument, Bragg-Bentano geometry, Cu K_α radiation, $2\theta = 5 - 20^\circ$, scan step size of 0.01°) and two-dimensional grazing incidence XRD (2D-GIXRD, Beamline 9 DELTA Synchrotron Germany, X-ray wavelength 1.0013 Å, incidence angle of 0.6° and refined sample-to-detector distance of 440.0 mm). Top and cross-sectional view scanning electron microscopic (SEM) images were taken by an environmental scanning electron microscope (ESEM, FEI ESEM Dual Beam™ Quanta 3D FEG) in order to investigate surface morphology and surface coverage of the MOF films. Methanol sorptions were carried out at controlled temperature of 25°C on an environmental-controlled quartz crystal microbalance (BEL-QCM-4 instrument, BEL Japan). The in-situ activation by heating at 80°C under dry He flow for 2 h was conducted prior to the measurements. After the activation process, the QCM frequency is recorded when the frequency change is stable within ±5 Hz in 20 min. Mass of the MOF films was calculated by the difference of the QCM frequency after activation and the fundamental frequency of the bare QCM substrates according to Sauerbrey's equation. Then, methanol sorption isotherms were collected by varying the relative vapor pressure (P/P_0) of saturated methanol vapor in He gas flow at 25°C from 0.0 to 95.0%. The adsorption amounts were also calculated according to Sauerbrey's equation.

Results and discussion

In order to evaluate the compatibility of the coordination modulation technique in LPE processing, its success in manipulating the growth of bulk crystals of the **Zn-L** structure type is firstly demonstrated. Then, the modulation process is integrated within the LPE deposition protocol of the same frameworks via addition of the modulator (*i.e.* acetic acid) during the metal dosing step. The influence of this procedure on the film properties is probed by way of comparison with films grown by the LPE process in the absence of the modulator. Finally, a number of detailed studies directed toward understanding the role of the modulator in the film growth process are described.

Preparation of bulk powders via coordination modulation

$Zn_4O(L)_3$ (Zn-L) structure type. Prior to discussion of the experimental results, the main structural and chemical features of the $Zn_4O(L)_3$ (**Zn-L**) structure type are presented. A portion of the structure of the **Zn-L** framework (shown for L^{2-} = 3,5-dimethyl-4-carboxypyrazolate; **Zn-DM**) is shown in Fig. 1A. The structure features tetrahedral $[Zn_4O]^{6+}$ units that are bound on average by three carboxylate and three pyrazolate moieties (Fig. 1B) that are bridged by the organic linkers to form a cubic network (space group: *Fm-3m*) isoreticular with the well-known $Zn_4O(bdc)_3$ (MOF-5, bdc^{2-} = benzene-1,4-dicarboxylate) framework. However, unlike MOF-5, the presence of the strongly binding pyrazolate moieties provides more robust metal-ligand bonding, and consequently a greater thermal and chemical stability.[25,26] Moreover, the size of the pore apertures is amenable to fine-tuning via changing the identity of the alkyl substituents on the pyrazolate ring. In this work, we employ the 3,5-dimethyl-4-carboxypyrazolate (DM^{2-}), 3-methyl-5-ethyl-4-carboxypyrazolate (ME^{2-}), and 3,5-diethyl-4-carboxypyrazolate (DE^{2-}) linkers shown in Fig. 1C to demonstrate the broad applicability of the coordination modulation technique to the **Zn-L** structure type.

Impact of coordination modulation on bulk powders. In conventional syntheses, the **Zn-L** frameworks are obtained by the reaction of $Zn(NO_3)_2{\cdot}6H_2O$ with the organic linker, H_2L, under reflux in a basic ethanol medium.[25] The same frameworks can be prepared by a ligand replacement reaction starting with a solution of pre-formed $Zn_4O(OAc)_6$ clusters, followed by addition of a linker solution to induce framework assembly.[26] Note that in this case, however, the obtained powders have a comparatively low crystallinity that, for the **Zn-DM** system, yields a significantly lower BET surface area[27] (470 m^2/g) compared to the conventional synthesis (840 m^2/g).[25]

Owing to its experimental convenience and previous successful implementation in the LPE-based deposition of other MOF systems, the ligand replacement approach was selected for further development and integration of the coordination modulation process. Here, the acetic acid modulator was incorporated into the metal cluster solution prior to combination with the organic linker, with the ratio of modulator relative to a fixed concentration of the organic linker (r_L) being varied from r_L = 1 to 30. An initial screening showed that in each of the three systems, **Zn-DM**, **Zn-ME**, and **Zn-DE**, the powder X-ray diffraction (PXRD) patterns confirmed the formation of the expected framework structure, but with increasing crystallinity with increasing r_L (see Fig. S1-S3).[28]

The enhanced crystallinity was also supported by scanning electron microscopy (SEM), which revealed an increase in the crystal size from the nanometer to micrometer regime, as well as the emergence of crystals exhibiting a well-defined cubic morphology (see Fig. S4-S6), upon increasing r_L. Notably, the BET surface area was significantly boosted upon introduction of the modulator to the synthetic protocol (see Table 1). In the case of **Zn-DM**, intermediate concentrations of the modulator (r_L = 3) optimized the BET surface area to a level even higher than that achieved via the conventional synthetic technique mentioned above (940 m^2/g), reinforcing the promise in integrating the coordination modulation technique in LPE-based processing of high-quality MOF thin-films.

Table 1. BET surface areas for **Zn-L** frameworks synthesized in bulk form with variation of the modulator-to-ligand ratio (r_L).

Compound	r_L	BET surface area ($m^2\ g^{-1}$)
Zn-DM	0	470
	1	740
	3	940
	5	920
Zn-ME	0	250
	2	670
Zn-DE	0	180
	1	210
	3	370

Integration of coordination modulation in the LPE-based fabrication of Zn-L films

LPE-based growth of Zn-DM. Given the success of coordination modulation in controlling the size and enhancing the properties of bulk crystals of **Zn-DM**, the analogous approach was then employed for LPE-based fabrication of thin-films of the same compound. In a typical preparation, the Au surface of a QCM substrate (pre-functionalized with a monolayer of 16-mercaptohexadecanoic acid (MHDA) to anchor the crystals) was alternatingly dosed with metal cluster and organic linker solutions in a continuous flow mode, with an ethanol washing step between precursor dosing stages. The QCM frequency change, which directly correlates with the mass of the deposited thin-film, was monitored in real-time to confirm the progress of film growth.[29] In a conventional LPE-based fabrication of **Zn-DM** (without modulator) the quantity of MOF deposited is observed to linearly increase with the cycling frequency.[27,30] Note that the **Zn-DM** compound and its analogues exhibit an island growth mode involving a relatively small number of initial MOF nuclei on the substrate surface, followed by subsequent growth into larger crystallites.[27,30] Although this facilitates the growth of **Zn-DM** films with micrometer thickness, the extent to which the crystal orientation and the overall film quality can be controlled is limited, highlighting a challenge associated with typical LPE processes.[27]

The influence of coordination modulation on thin-film growth was then tested by varying the concentration of the modulator relative to the concentration of $Zn_4O(OAc)_6$ in the metal precursor solution (expressed via the ratio r_M) in an otherwise identical LPE-based process. Note that for the LPE-based fabrication, the parameter r_M is more relevant than r_L as described for bulk syntheses, since the modulator is added to the metal precursor solution and a washing step exists between metal and organic linker dosing steps. The QCM data stemming from deposition processes using r_M values ranging from 0 to 5 is presented in Fig. 2. In all cases, the quantity of **Zn-DM** deposited on the substrate increased as a function of the cycling frequency, as reflected by the decrease in oscillation frequency (F) as a function of time.[29] However, the quantity deposited *per step* was significantly affected by r_M, which is ascribed to the modulator influencing the nucleation and growth phases of thin-film growth.

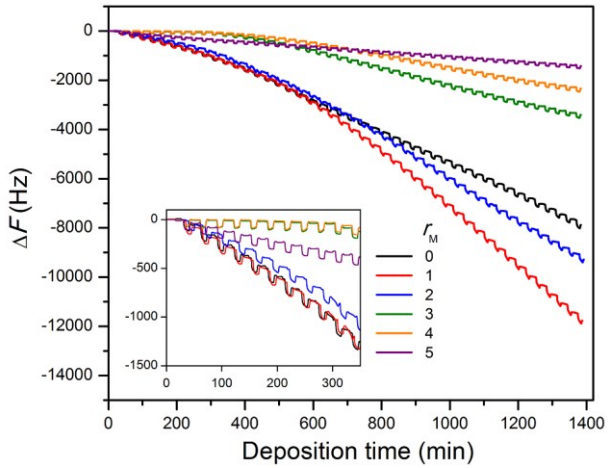

Fig. 2 Plots showing changes in the QCM oscillator frequency (F) as a function of time during the fabrication of **Zn-DM** films with variation of the modulator-to-metal ratio (r_M).

Closer inspection of the QCM frequency data revealed that, in the initial stages of deposition (<10 deposition cycles; Fig. 2, inset), the quantity of MOF grown on the surface was significantly reduced for $r_M \geq 3$, suggesting the disruption of the initial nucleation process (as observed in the case of bulk MOF systems) at high modulator concentrations.[16,17] At lower levels ($r_M \leq 2$), the influence of the modulator was found to be limited over the same period. However, beyond this nucleation stage (Fig. 2, main panel), the deposited mass per deposition cycle was enhanced for r_M = 1 and 2, as indicated by the steeper (negative) slope in the frequency change profile relative to the conventional process (r_M = 0). This can be rationalized by the fact that larger crystals are likely to emerge upon addition of the modulator, whose growth surfaces, at which additional metal clusters and ligand molecules can attach to effect further growth, will be larger than in the absence of modulator. Thus, the limited perturbation of the initial nucleation at low modulator concentrations coupled with growth of larger crystallites leads to more rapid growth of these films over the timeframe studied. At higher modulator concentrations ($r_M \geq 3$), the significant disruption to the nucleation process leads to fewer available growth sites, leading to slower overall growth and a lower mass of material deposited on the surface. Note that, while the QCM platform provides a highly sensitive quantitative method of observing the deposition of thin-films, it does not provide information regarding the composition or morphology of the materials. Thus, full characterization of the films was carried out in order to ascertain the influence of the modulator on the film growth and characteristics of the films.

View Article Online DOI: 10.1039/C7TA02848B

Characterization of thin-films. Detailed analysis of the composition of the deposited films were carried out via PXRD experiments (see Fig. 3). In each case, a good match with the simulated pattern of bulk **Zn-DM** was obtained, indicating phase-pure **Zn-DM** was deposited on the QCM substrate surface. Interestingly, the addition of modulator during the deposition led to a pronounced preferred crystal orientation in the [100] direction, as evidenced by an increased intensity in the *h00* reflections. In contrast, the **Zn-DM** films fabricated in the absence of the modulator (r_M = 0) showed the remainder of the expected diffraction peaks (e.g. *220* and *311*), which is consistent with a random orientation of the crystallites. To probe the orientation of the films further, two-dimensional grazing incidence X-ray diffraction (2D-GIXRD) data were collected for a **Zn-DM** films fabricated using r_M = 0 and 2 (Fig. 4, see also Fig. S10). In the absence of the modulator (Fig. 4A), the broad ring-like profile of the diffraction peaks is indicative of a limited control over the growth orientation of the crystals. However, the incorporation of the modulator during growth revealed discrete reflections in the corresponding data (Fig. 4B), which indicate that the films are oriented in the film growth direction (normal to the substrate surface). This ability to tune both the crystallinity and crystal orientation illustrate a clear advantage of incorporating coordination modulation in an LPE-based fabrication protocol.

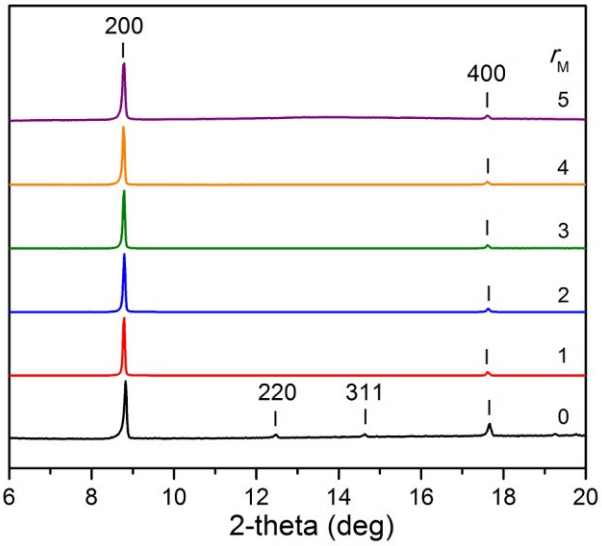

Fig. 3 Powder X-ray diffraction (PXRD) patterns of the **Zn-DM** films fabricated by the LPE process with variation of the modulator-to-metal ratio (r_M).

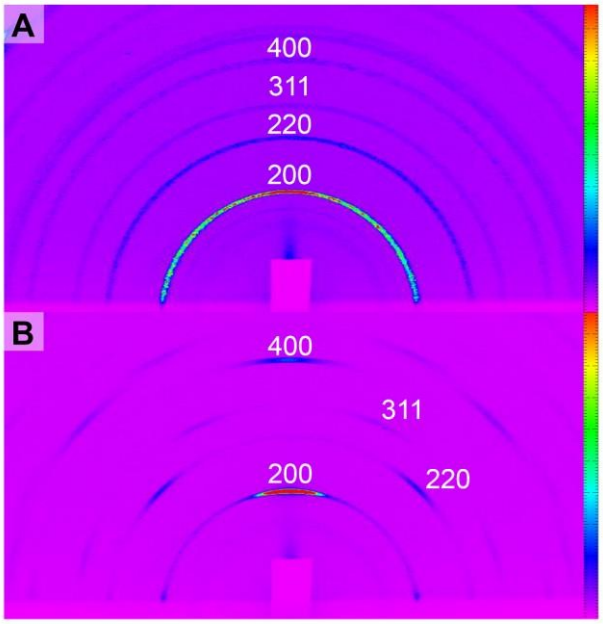

Fig. 4 Two-dimensional grazing-incidence X-ray diffraction (2D-GIXRD) patterns collected for **Zn-DM** films fabricated using modulator-to-metal ratios (r_M) of (A) 0; and (B) 2 (source parameters: wavelength 1.0013 Å, incidence angle 0.6, refined sample-to-detector distance 440.0 mm). The color of each pixel reflects the diffraction intensity from low (magenta) to high (red).

To further probe the influence of coordination modulation on the crystal orientation and morphology of the deposited MOF thin-films, top (Fig. 5) and cross-sectional (Fig. S11) views of the **Zn-DM** films were obtained via scanning electron microscopy (SEM). In the absence of the modulator (Fig. 5A), crystals with square facets are observed with a broad range of crystal sizes and orientations. This reflects the limitation of control over the nucleation and crystal growth using a conventional LPE-based fabrication process. However, addition of a small amount of modulator (r_M = 1 and 2) led to the formation of larger, square plate-like crystals with a denser packing and consistent orientation (Fig. 5B and C). Further increases in the modulator concentration ($r_M \geq 3$) led to a reduction in the crystal size and an incomplete surface coverage (Fig. 5D to F). These observations are consistent with the QCM frequency data presented in Fig. 2, which displayed the most rapid overall deposition of the film for r_M = 1 and 2, and reduced nucleation and growth at $r_M \geq 3$.

The influence of coordination modulation on the films fabricated by the LPE-based protocol was tested via methanol adsorption experiments. Here, a helium gas flow containing a controlled partial pressure of methanol vapor was introduced to a QCM cell held at a constant temperature of 25 °C, and the mass of methanol adsorbed was recorded following stabilization of the substrate frequency. The methanol adsorption data for the **Zn-DM** thin-films fabricated using different r_M values is presented in Fig. 6A. Addition of modulator during the film fabrication process enhanced the methanol adsorption capacity from 7.40 mmol/g (r_M = 0) to 10.43 mmol/g (r_M = 2) at P/P_0 = 0.95 (Fig. 6A), which is likely a direct consequence of the enhanced crystallinity and packing of the film, and a decrease in the amount of amorphous, non-porous phases and low-porosity regions of the MOF film. The adsorption capacity is maximized in the range of r_M = 2 to 4, after which the capacity decreases due to a significantly lower micropore density, which may be associated with lower-quality pore formation associated with a significantly smaller crystal size compared to the other samples examined in these experiments.[31]

LPE-based growth of Zn-ME. A similar optimization procedure was carried out using the organic linker H_2ME (see Fig. 1C) to

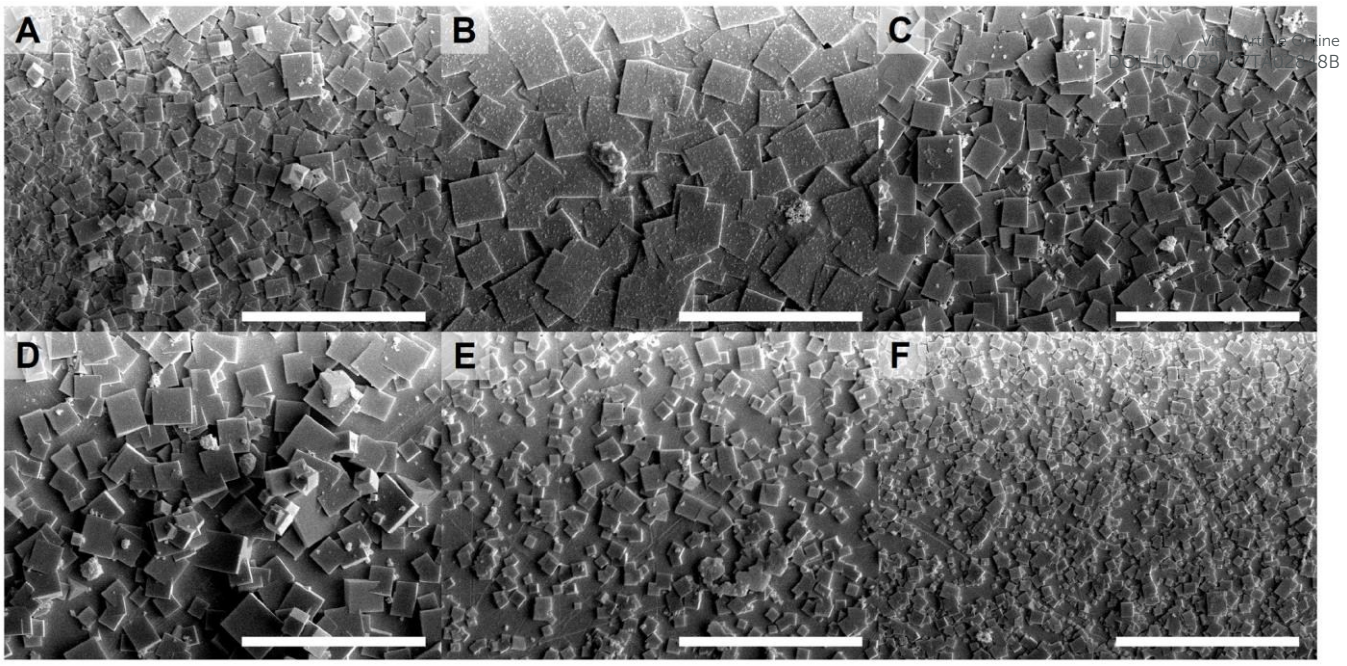

Fig. 5 SEM images of the surfaces of **Zn-DM** films fabricated using modulator-to-metal ratios (r_M) of (A) 0; (B) 1; (C) 2; (D) 3; (E) 4; and (F) 5. The scale bar at the bottom right of each panel represents a length of 10 μm.

test the utility of coordination modulation with respect to the LPE-based fabrication of other members of the **Zn-L** structure type. The analogous deposition protocol in the absence of the modulator (r_M = 0) led to the expected formation of **Zn-ME** as indicated by PXRD (Fig. S14), and SEM data (Fig. S15 and S16) revealed the appearance of square, plate-like crystals approximately 1 μm in size. Introduction of the modulator during the deposition process enhanced the orientation of the films, as demonstrated by the discrete reflections in the 2D-GIXRD data shown in Fig. S17. Further, although less pronounced relative to the case of **Zn-DM**, the enhanced crystallinity and preferred orientation resulted in a marginal enhancement in the adsorption capacity of methanol (increase of 15% for r_M = 3 at P/P_0 = 0.95 relative to the r_M = 0 case, see Fig. S18), which further confirms the benefit of the addition of a small quantity of a modulator during the film growth.

LPE-based growth of Zn-DE. The deposition of the **Zn-DE** framework could also be readily optimized via the same fabrication protocols using the linker H_2DE (see Fig. 1C). In a similar manner to both **Zn-DM** and **Zn-ME**, a conventional LPE-based deposition process afforded the expected **Zn-DE** framework (Fig. S19), which exhibited a square plate-like morphology (Fig. S20) and dense film packing (Fig. S21). The addition of small quantities of modulator (up to r_M = 3) provided enhanced crystallinity and film orientation as confirmed by 2D-GIXRD data (Fig. S22). Interestingly, upon characterization of the adsorption properties of the films, a considerable enhancement in the methanol adsorption capacity was observed for films derived using r_M = 2 and 3, which exhibited increases of 69% and 120% at P/P_0 = 0.95 relative to the r_M = 0 case, respectively (Fig. 6B). This boost in adsorption capacity, and overall benefit of the coordination modulation approach, is likely particularly pronounced compared to the other

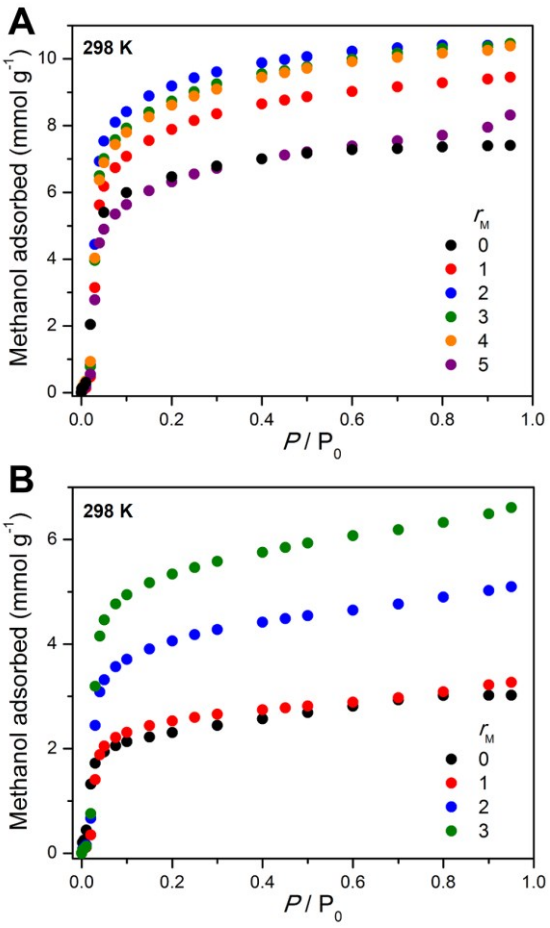

Fig. 6 Methanol adsorption data collected using an environment-controlled QCM at 298 K for (A) **Zn-DM**; and (B) **Zn-DE** films fabricated using varying modulator-to-metal ratios (r_M).

frameworks due to the more sterically demanding nature of the organic linker (possessing two ethyl groups on the pyrazolate backbone, rather than methyl groups), where the overall properties are more sensitive to blockages and pore clogging as a result of lattice defects or low-crystallinity portions of the film. Thus, the enhanced crystallinity and preferred orientation of the films fabricated in the presence of the modulator (and elimination of low-porosity components with little or no crystallinity) facilitates the formation of more periodic, uniform pores, which in turn allows the surface area to be maximized. In all, for **Zn-DM**, **Zn-ME** and **Zn-DE**, the use of coordination modulation during the metal dosing step provides enhancements in the film properties, highlighting the success of this approach.

Probing the role of coordination modulation in optimizing LPE fabrication

Film nucleation and growth. The success of the coordination modulation approach in enhancing the growth rate and properties of the **Zn-L** films prompted more detailed investigation regarding the influence of the modulator on the molecular interactions during the fabrication process. Here, the fact that the modulator is present within the metal-containing solution suggested its importance on the metal dosing step of the fabrication process, and hence it was postulated that variation of the value of r_M exerts changes in the affinity of $[Zn_4O]^{6+}$ clusters toward the substrate surface via manipulations of a solution equilibrium of the type shown in Equation 1. In such a system, there is an equilibrium between $Zn_4O(OAc)_6$ molecules in the bulk solution and those that are bound to carboxylate moieties of the organic ligands or the initially deposited carboxylate-terminated SAM (denoted by $L_{surface}$). The binding of the cluster to $L_{surface}$ liberates an acetic acid molecule, and hence the addition of excess modulator molecules is expected to shift this equilibrium toward the reactants, resulting in less metal binding to the surface. This is expected to contribute to lower initial crystal nucleation, and slower overall film growth as observed in the QCM data in Fig. 2.

$$Zn_4O(OAc)_6 + HL_{surface} \rightleftharpoons [Zn_4O(OAc)_5]L_{surface} + AcOH \quad (1)$$

In order to probe this effect, a metal solution without modulator (r_M = 0) was firstly delivered to the QCM surface to facilitate the attachment of $[Zn_4O]^{6+}$ clusters to the substrate. This was then followed by treatment of the substrate with a modulator solutions of various concentrations (0.5, 1.0, and 2.0 mM in ethanol), and the relative quantities of the metal clusters attached to the surface upon reaching equilibrium were analyzed by the frequency changes in the quartz oscillator. Fig. 7 illustrates the QCM data for the three modulator concentrations collected over four cycles (where each cycle represents metal dosing, followed by treatment with the modulator solution). At the lower concentrations of 0.5 (red) and 1.0 (blue) mM, the switching of the treatment solution from the metal solution to the modulator solution (indicated by the vertical red dashed lines in Fig. 7) resulted in minimal changes

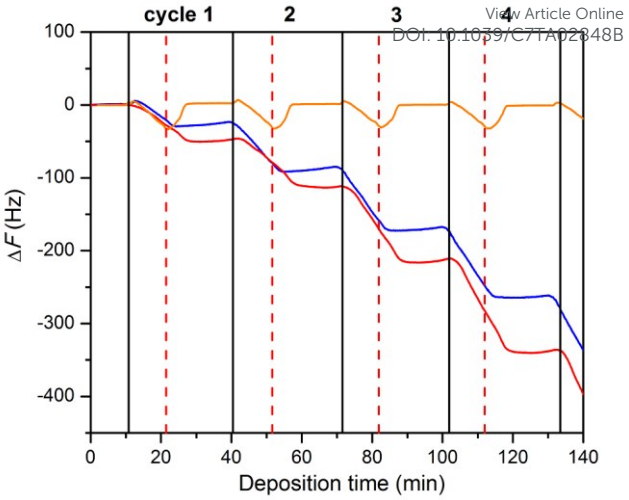

Fig. 7 QCM data showing frequency changes of the oscillator as a function of time over four metal dosing cycles. Here, each cycle represents the treatment of the substrate with a metal solution (0.5 mM), followed by washing using modulator-containing solutions having concentrations of 0.5 mM (red), 1.0 mM (blue), and 2.0 mM (red). The beginning and end of each cycle is represented by vertical solid black lines, while the timing of the modulator addition is indicated by the vertical dashed red lines.

in the frequency, indicating that the metal clusters were retained on the surface. However, upon increasing the modulator concentration to 2.0 mM (orange), which approximately correlates with r_M = 4 in the fabrication studies described above, a complete detachment of the surface-bound $Zn_4O(OAc)_6$ clusters from the substrate is observed due to the frequency returning to the baseline. Therefore, higher modulator concentrations restrict the quantity of metal cluster deposition on the substrate surface, which in turn reduces crystal nucleation and opportunities for film growth. This is consistent with the trends in the rate of overall deposition of the **Zn-L** films as shown above (Fig. 2), which demonstrates that precise tuning of the modulator concentration can achieve control over the film growth rate via tuning of the quantity of the metal cluster deposited on the film surface.

Film crystallinity and preferred orientation. As shown above, the rate of the initial stages of film growth is highly dependent on the concentration of the modulator, which is directly correlated to the quantity of the metal cluster that is deposited on the growth surface. Since the **Zn-L** films deposited in presence of the modulator also feature enhanced crystallinity and orientation, this suggested that the first few growth cycles also play an important role in determining these features of the product film. In order to probe this in more detail, the properties of a **Zn-DM** film prepared by via a conventional LPE process (r_M = 0) for the first five cycles followed by further growth in the presence of the modulator were compared with those employing coordination modulations for all deposition cycles of the fabrication process. The 2D-GIXRD patterns in the former case exhibited a small *220* diffraction peak in the out-of-plane direction (90° line cut), illustrating a more randomized

orientation of the MOF crystals along the film growth direction (Fig. S26). This confirms that the presence of the modulator in the initial deposition cycles is crucial in determining the crystal orientation of the resulting films, and reveals that the quality of the nucleation process is propagated to the uniformity of the orientation of product films despite the use of coordination modulation in the later stages of film fabrication.

The influence of modulator addition to organic linker solutions, rather than the metal solutions, was also probed to ascertain whether the enhancement in film properties is unique to protocols incorporating the modulator in the metal deposition step of the LPE process. Interestingly, in all cases where the modulator was incorporated in organic linker solutions, *220* and *311* diffraction peaks were observed in the PXRD patterns (Fig. S30), indicating a reduced uniformity in the crystal orientation. Further, these films displayed no significant enhancement in their methanol adsorption capacity, suggesting that the quality is not enhanced above those prepared in the absence of the modulator (Fig. S31). This indicates that the presence of the modulator during metal cluster deposition is crucial in order to achieve high-quality **Zn-DM** films. Although detailed molecular-level insights of the origins of this observation are not yet available, it is likely that only the most strongly bound, and therefore the most thermodynamically stable, conformations of cluster binding on the surface are present in upon addition of the modulator (i.e. weaker, loosely bound clusters are removed from the surface). This presumably reduces the number of possible coordination modes of the cluster on the surface, which allows the films to grow in a more uniform and oriented fashion.

Conclusions

The foregoing has demonstrated that the integration of coordination modulation with an LPE-based fabrication protocol can provide a significant enhancement in the quality of MOF-based thin films. In the **Zn-L** system investigated in this study, addition of even small quantities of a modulator during the metal dosing step has been demonstrated as being beneficial in achieving more crystalline and oriented, high-density MOF thin-films. Such enhancements are expected to be crucial in applications such as molecular sensing, where higher film quality can directly enhance detection limits, response times, estimation of analyte concentrations, and device lifetimes. It is expected that, in a similar fashion to the preparation of bulk MOF crystals, coordination modulation will be applicable to LPE-based thin-film deposition protocols of a wide variety of MOF structure types. The current challenge lies in more fully understanding the molecular interactions that dictate the final properties of the film, and studies that address the deposition of a greater variety of MOFs using a broader scope of modulator types are currently underway.

Acknowledgements

This work was initially supported by Priority Program 1362 "Metal-Organic Frameworks", and later by the Cluster of Excellence RESOLV (EXC 1069) funded by the German Research Foundation (DFG). iCeMS is supported by the World Premier International Research Initiative (WPI), MEXT, Japan. DELTA is acknowledged for use of beamline BL09 for grazing incidence X-ray diffraction measurements. S. W. thanks the Royal Thai Government under the Ministry of Science and Technology for a Ph.D. scholarship, and the International Realization Budget (IRB) of the Research School Plus, Ruhr-University Bochum (GSC 98) for international travel and research funding. K. S. thanks the JSPS Postdoctoral Fellowship for Foreign Researchers (P12040), and the Australian Research Council (DE160100306) for funding. We thank Dr C. Sternemann and Dr M. Paulus of DELTA for experimental assistance and Dr R. Medishetty at the Chair of Inorganic and Metal-Organic Chemistry, Department of Chemistry, TUM for helpful discussions.

Notes and references

1 a) H.-C. Zhou, J. R. Long and O. M. Yaghi, *Chem. Rev.*, 2012, **112**, 673; b) H.-C. Zhou and S. Kitagawa, *Chem. Soc. Rev.*, 2014, **43**, 5415.

2 a) O. M. Yaghi, M. O'Keeffe, N. W. Ockwig, H. K. Chae, M. Eddaoudi and J. Kim, *Nature*, 2003, **423**, 705; b) S. Kitagawa, R. Kitaura and S.-i. Noro, *Angew. Chem. Inter. Ed.*, 2004, **43**, 2334; c) G. Ferey, *Chem. Soc. Rev.*, 2008, **37**, 191.

3 a) K. Sumida, D. L. Rogow, J. A. Mason, T. M. McDonald, E. D. Bloch, Z. R. Herm, T.-H. Bae and J. R. Long, *Chem. Rev.*, 2012, **112**, 724; b) M. P. Suh, H. J. Park, T. K. Prasad and D.-W. Lim, *Chem. Rev.*, 2012, **112**, 782; c) R. B. Getman, Y.-S. Bae, C. E. Wilmer and R. Q. Snurr, *Chem. Rev.*, 2012, **112**, 703; d) E. Barea, C. Montoro and J. A. R. Navarro, *Chem. Soc. Rev.*, 2014, **43**, 5419; e) Y. He, W. Zhou, G. Qian and B. Chen, *Chem. Soc. Rev.*, 2014, **43**, 5657.

4 a) J.-R. Li, J. Sculley and H.-C. Zhou, *Chem. Rev.*, 2012, **112**, 869; b) B. van de Voorde, B. Bueken, J. Denayer and D. de Vos, *Chem. Soc. Rev.*, 2014, **43**, 5766.

5 a) A. Dhakshinamoorthy and H. Garcia, *Chem. Soc. Rev.*, 2014, **43**, 5750; b) M. Yoon, R. Srirambalaji and K. Kim, *Chem. Rev.*, 2012, **112**, 1196.

6 V. Stavila, A. A. Talin and M. D. Allendorf, *Chem. Soc. Rev.*, 2014, **43**, 5994.

7 P. Ramaswamy, N. E. Wong and G. K. H. Shimizu, *Chem. Soc. Rev.*, 2014, **43**, 5913.

8 T. Zhang and W. Lin, *Chem. Soc. Rev.*, 2014, **43**, 5982.

9 L. E. Kreno, K. Leong, O. K. Farha, M. Allendorf, R. P. van Duyne and J. T. Hupp, *Chem. Rev.*, 2012, **112**, 1105.

10 a) Z. Hu, B. J. Deibert and J. Li, *Chem. Soc. Rev.*, 2014, **43**, 5815; b) Y. Cui, Y. Yue, G. Qian and B. Chen, *Chem. Rev.*, 2012, **112**, 1126.

11 a) R. Ricco, C. Pfeiffer, K. Sumida, C. J. Sumby, P. Falcaro, S. Furukawa, N. R. Champness and C. J. Doonan, *CrystEngComm*, 2016, **18**, 6532; b) P. Horcajada, R. Gref, T.

Baati, P. K. Allan, G. Maurin, P. Couvreur, G. Férey, R. E. Morris and C. Serre, *Chem. Rev.*, 2012, **112**, 1232.

12 a) S. Furukawa, J. Reboul, S. Diring, K. Sumida and S. Kitagawa, *Chem. Soc. Rev.*, 2014, **43**, 5700; b) P. Falcaro, R. Ricco, C. M. Doherty, K. Liang, A. J. Hill and M. J. Styles, *Chem. Soc. Rev.*, 2014, **43**, 5513; K. Sumida, K. Liang, J. Reboul, I. A. Ibarra, S. Furukawa and P. Falcaro, *Chem. Mater.*, 2017, DOI: 10.1021/acs.chemmater.6b03934.

13 a) L. Heinke, M. Tu, S. Wannapaiboon, R. A. Fischer and C. Wöll, *Microporous Mesoporous Mat.*, 2015, **216**, 200; b) M. Tu, S. Wannapaiboon and R. A. Fischer, *Inorg. Chem. Front.*, 2014, **1**, 442; c) L. Heinke, H. Gliemann, P. Tremouilhac and C. Wöll, *The Chemistry of Metal–Organic Frameworks: Synthesis, Characterization, and Applications*, Wiley-VCH, Weinheim, Germany, 2016, pp. 523–550.

14 a) O. Shekhah, H. Wang, S. Kowarik, F. Schreiber, M. Paulus, M. Tolan, C. Sternemann, F. Evers, D. Zacher, R. A. Fischer and C. Wöll, *J. Am. Chem. Soc.*, 2007, **129**, 15118; b) O. Shekhah, H. Wang D. Zacher, R. A. Fischer and C. Wöll, *Angew. Chem. Inter. Ed.*, 2009, **48**, 5038; c) D. Zacher, K. Yusenko, A. Bétard, S. Henke, M. Molon, T. Ladnorg, O. Shekhah, B. Schüpbach, T. de los Arcos, M. Krasnopolski, M. Meilikhov, J. Winter, A. Terfort, C. Wöll and R. A. Fischer, *Chem. Eur. J.*, 2011, **17**, 1448; d) O. Shekhah, H. K. Arslan, K. Chen, M. Schmittel, R. Maul, W. Wenzel and C. Wöll, *Chem. Commun.*, 2011, **47**, 11210; e) B. Liu, M. Tu, D. Zacher and R. A. Fischer, *Adv. Funct. Mater.*, 2013, **23**, 3790; f) M. Tu, S. Wannapaiboon and R. A. Fischer, *Dalton Trans.*, 2013, **42**, 16029; g) Z. Wang, J. Liu, B. Lukose, Z. Gu, P. G. Weidler, H. Gliemann, T. Heine and C. Wöll, *Nano Lett.*, 2014, **14**, 1526; h) L. Heinke, M. Cakici, M. Dommaschk, S. Grosjean, R. Herges, S. Bräse and C. Wöll, *ACS Nano*, 2014, **8**, 1463.

15. T. Tsuruoka, S. Furukawa, Y. Takashima, K. Yoshida, S. Isoda and S. Kitagawa, *Angew. Chem. Inter. Ed.*, 2009, **48**, 4739.

16 A. Umemura, S. Diring, S. Furukawa, H. Uehara, T. Tsuruoka and S. Kitagawa, *J. Am. Chem. Soc.*, 2011, **133**, 15506.

17 S. Diring, S. Furukawa, Y. Takashima, T. Tsuruoka and S. Kitagawa, *Chem. Mater.*, 2010, **22**, 4531.

18 Y. Sakata, S. Furukawa, M. Kondo, K. Hirai, N. Horike, Y. Takashima, H. Uehara, N. Louvain, M. Meilikhov, T. Tsuruoka, S. Isoda, W. Kosaka, O. Sakata and S. Kitagawa, *Science*, 2013, **339**, 193.

19 a) J. Cravillon, R. Nayuk, S. Springer, A. Feldhoff, K. Huber and M. Wiebcke, *Chem. Mater.*, 2011, **23**, 2130; b) N. Yanai, M. Sindoro, J. Yan and S. Granick, *J. Am. Chem. Soc.*, 2013, **135**, 34; c) J. Cravillon, C. A. Schroder, H. Bux, A. Rothkirch, J. Caro and M. Wiebcke, *CrystEngComm*, 2012, **14**, 492.

20 a) A. Schaate, P. Roy, A. Godt, J. Lippke, F. Waltz, M. Wiebcke and P. Behrens, *Chem. Eur. J.*, 2011, **17**, 6643; b) H. Fei, S. Pullen, A. Wagner, S. Ott and S. M. Cohen, *Chem. Commun.*, 2015, **51**, 66.

21 G. Zahn, P. Zerner, J. Lippke, F. L. Kempf, S. Lilienthal, C. A. Schroder, A. M. Schneider and P. Behrens, *CrystEngComm*, 2014, **16**, 9198.

22 H. Guo, M. Wang, J. Liu, S. Zhu and C. Liu, *Microporous Mesoporous Mat.*, 2016, **221**, 40.

23 D. Feng, K. Wang, Z. Wei, Y.-P. Chen, C. M. Simon, R. K. Arvapally, R. L. Martin, M. Bosch, T.-F. Liu, S. Fordham, D. Yuan, M. A. Omary, M. Haranczyk, B. Smit and H.-C. Zhou, *Nat. Commun.*, 2014, **5:5723**.

24 H. Uehara, S. Diring, S. Furukawa, Z. Kalay, M. Tsotsalas, M. Nakahama, K. Hirai, M. Kondo, O. Sakata and S. Kitagawa, *J. Am. Chem. Soc.*, 2011, **133**, 11932.

25 C. Montoro, F. Linares, E. Quartapelle Procopio, I. Senkovska, S. Kaskel, S. Galli, N. Masciocchi, E. Barea and J. A. R. Navarro, *J. Am. Chem. Soc.*, 2011, **133**, 11888.

26 A. Betard, S. Wannapaiboon and R. A. Fischer, *Chem. Commun.*, 2012, **48**, 10493.

27 S. Wannapaiboon, M. Tu and R. A. Fischer, *Adv. Funct. Mater.*, 2014, **24**, 2696.

28 Note that, beyond certain levels of modulator addition ($r_L = 7$ for **Zn-DM**, $r_L = 3$ for **Zn-ME** and **Zn-DE**), an uncharacterized impurity phase emerges, which potentially arises due to the more prevalent modulator component affecting carboxylate and pyrazolate binding unequally, thereby leading to anisotropic (and lower-symmetry) phases becoming the preferred product.

29 A mass based on a frequency change of the quartz oscillator is obtained based on the Sauerbrey's equation as follows: $\Delta F = - (2F_0^2/A\cdot(\mu\cdot\rho)^{1/2}) \cdot \Delta M$, where F_0 : fundamental frequency of QCM sensor, A : surface area of electrode, μ : shear stress of quartz (2.947×10^{10} kg·m^{-1}·s^{-2}) and ρ : density of quartz (2648 kg·m^{-3})

30 S. Wannapaiboon, M. Tu, K. Sumida, K. Khaletskaya, S. Furukawa, S. Kitagawa and R. A. Fischer, *J. Mater. Chem. A*, 2015, **3**, 23385.

31 Note that the introduction of non-periodic defects (*e.g.* linker absences) can also boost the adsorption capacity of MOFs in some cases. However, infrared spectroscopy (Fig. S13) revealed little difference in composition for samples fabricated at different r_M values, while the pore size distributions also appeared unchanged based on the similarity in the form of the adsorption profiles and the kinetic (diffusion) data for methanol adsorption (Fig. S12, S18 and S23). Therefore, the boost in adsorption capacity presumably arise via the elimination of low-crystallinity or amorphous portions of the film that accommodate a lower gravimetric capacity for guest molecules compared to the pristine regions of the MOF film.

View Article Online
DOI: 10.1039/C7TA02848B

Table of contents

Enhanced Properties of Metal-Organic Framework Thin-Films Fabricated via a Coordination Modulation-Controlled Layer-by-Layer Process

Suttipong Wannapaiboon,[a,b] Kenji Sumida,[c,d,*] Katharina Dilchert,[b] Min Tu,[b,e] Susumu Kitagawa,[c] Shuhei Furukawa[c] and Roland A. Fischer[a,*]

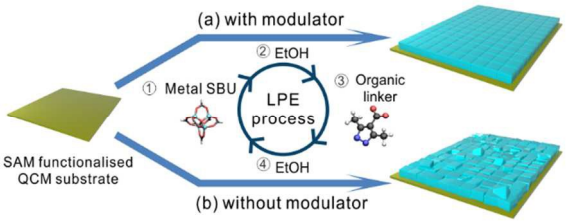

Addition of the modulator in LPE process enhances MOF thin-film properties by boosting their crystallinity, orientation uniformity, and adsorptive capacity.